

Compact spectroscopy system based on tunable organic semiconductor lasers

T. Woggon · S. Klinkhammer · U. Lemmer

Received: 8 January 2010 / Revised version: 18 February 2010 / Published online: 6 March 2010
© Springer-Verlag 2010

Abstract We applied a continuously tunable organic semiconductor thin film laser for high resolution transmission spectroscopy. Using a suitable encapsulation application of that low-cost laser device allowed us to realize a very compact and durable measurement system incorporating only very few optical components. To demonstrate the capability of our setup for high-resolution photospectroscopy, we measured the transmission curve of a narrow laser line filter. The resulting data was in good agreement with a measurement of the filter characteristic done using a commercial spectrometer. Our system is capable of measuring optical density (OD) values up to OD 5. A key for future systems is a novel low-cost mechanical tuning method for position-dependent distributed feedback lasers which enables high-speed tuning with wavelength access times under 10 ms independent of the tuning bandwidth.

1 Introduction

The field of organic distributed feedback (DFB) semiconductor lasers has attracted great interest among the research community since the first publications [1] because of their numerous advantages over their inorganic counterparts [2, 3]. Their key benefits are low-cost fabrication methods while maintaining the possibility to tailor the emission wavelength on demand [4, 5]. Organic lasers with

emission wavelengths over the whole visible spectral region [6–9] have been demonstrated as well as continuously tunable devices [10]. Additionally, low-threshold organic lasers pumped by a single laser diode or even a light-emitting diode have been shown [11–13]. There has also been progress made on integrating organic lasers for lab-on-a-chip applications [14]. However, despite these research progresses made over recent years the lack of applications is still holding back the commercial breakthrough of organic semiconductor lasers. The reasons for that are mainly degradation issues due to photo-oxidation or low output powers that are considered to be too weak for reasonable measurements. Here we demonstrate that organic semiconductor lasers are mature enough for applications in spectroscopy. For this purpose we built a compact optical transmission spectrometer based on a continuously tunable organic distributed feedback laser. The system consists of only a limited number of components. With this system we were able to conduct optical transmission spectroscopy with a spectral resolution and sensitivity comparable to a commercial spectrophotometer. Tuning of the laser wavelength is accomplished by pumping at different spatial positions of a monomode waveguide with varying thickness, which translates into a position-dependent laser wavelength. We show rapid mechanical tuning of such a pump position dependent laser using a spinning disc approach. The setup allows tuning of the laser wavelength within milliseconds and is based on a low-cost hardware solution.

2 Experimental

In prior work Klinkhammer et al. proposed laser interference lithography in combination with a rotating shadow mask evaporation technique for the fabrication of widely

T. Woggon (✉) · S. Klinkhammer · U. Lemmer
Light Technology Institute and Center for Functional
Nanostructures (CFN), Karlsruhe Institute of Technology (KIT),
76131 Karlsruhe, Germany
e-mail: thomas.woggon@kit.edu
Fax: +49-721-6082590

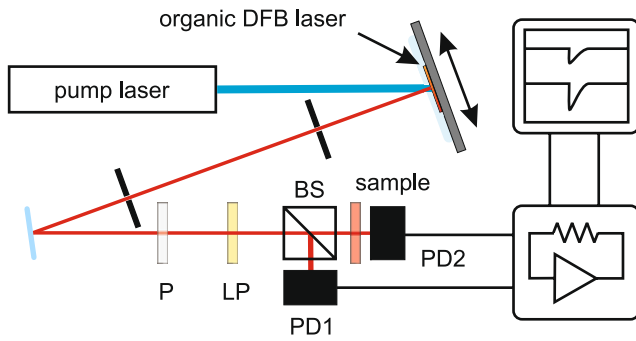


Fig. 1 Schematic of the optical setup and the detection scheme

tunable organic semiconductor lasers [10]. For the experiment, we used this method to fabricate a DFB laser sample with a continuous tuning range of more than 10 nm. For the resonator we textured a glass substrate with a one-dimensional second-order distributed Bragg reflector surface grating using laser interference lithography [15] and reactive ion etching. Optical confinement and gain are provided by a wedge-shaped layer of the organic semiconductor tris(8-hydroxyquinoline) aluminum doped with 2.5 mol% of the laser dye 4-dicyanomethylene-2-methyl-6-(p-dimethylaminostyryl)-4H-pyrene, which was fabricated with a rotating shadow mask evaporation. To protect the laser device from environmental influences, it was encapsulated under a pure nitrogen atmosphere. This was accomplished by putting the sample on an aluminum back plate and bonding a petri dish under nitrogen atmosphere on top with an epoxy resin. Figure 1 shows a schematic of our optical setup. The organic laser is optically pumped by an actively Q-switched frequency-tripled neodymium-doped yttrium lithium fluoride laser (Newport Explorer Scientific) with an emission wavelength of 349 nm at a repetition rate of 100 Hz. The resulting pump pulse energy is adjustable between 5 and 30 μJ . A straightforward way of tuning the organic laser's emission wavelength is achieved by moving the sample relative to the pump laser beam using a linear positioning stage. The stage is equipped with a Newport 850G actuator controlled by a Newport ESP300 motion controller yielding a position accuracy of better than one micron. The organic laser emission is directed through a polarizer (P) in order to select between TE and TM modes and a 385-nm long-pass filter (LP) to eliminate residual pump laser light. Subsequently, the beam is split into a probe and a reference beam using a polarization-insensitive 50:50 beam splitter (BS, Thorlabs CM1-BS1). The probe and reference beam were detected with single-pulse resolution using two silicon photodiodes (PDs) which were connected to a 200-MHz oscilloscope (Tektronix TDS 2024) using two transimpedance amplifiers with a transfer ratio of 1 V/nA. As a one-dimensional DFB laser at higher pump energies emits multiple lateral laser modes at different angles φ [16],

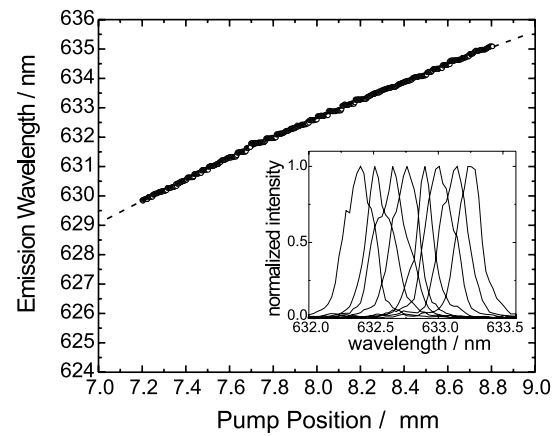


Fig. 2 Emission wavelength calibration in relation to the excitation spot position for the organic semiconductor laser. The curve data is discretized in approx. 0.03-nm steps due to the limited resolution of the spectrometer. The inset shows a selection of the respective laser spectra

we used two 0.8-mm apertures for mode selection and alignment. This is essential as it ensures that the two photodiodes are exposed to the same lateral mode. The pump position dependent ratio between the probe and reference photodiode readings was recorded with a computer. This transmission spectrophotometer was calibrated by measuring the pump position dependent emission wavelength using a 300-mm spectrograph with a resolution of 0.1 nm (SpectraPro 300i, Acton Research, 1200 g/mm grating). The resulting relation for a displacement step size of 2 μm is shown in Fig. 2. Due to the limited resolution of the spectrometer, the data curve is discretized in steps of approx. 0.03 nm. We fitted a second-order polynomial function to the data and used the result for the following measurements.

To test our system, we measured the transmission spectrum of a (632.8 ± 0.2) nm laser line filter with a full width at half maximum (FWHM) of (1 ± 0.2) nm (Thorlabs FL632.8-1). The result after applying zero and baseline corrections to the measurement data is the curve plotted as a solid line in Fig. 3. The curve peak is at 632.7 nm with a transmission value of 0.71 and a FWHM of 1.16 nm. We evaluated the quality of our measurement by taking the transmission spectrum of the filter using a commercial spectrophotometer (Varian Cary 5 VIS). In the instrument's settings we chose the data interval to the smallest available value of 0.005 nm for optimal results. The spectral bandwidth was set to a fixed value of 0.025 nm and we used the reduced slit height setting to minimize the divergence of the incident beam. An integration time of 500 ms assured a low noise signal [17]. The result is plotted as a dashed line in Fig. 3 with a peak wavelength of 632.74 nm and a FWHM of 1.2 nm. It can be seen that considering the measuring accuracy both measurements are in good agreement. We determined the sensitivity of our system by measuring the ab-

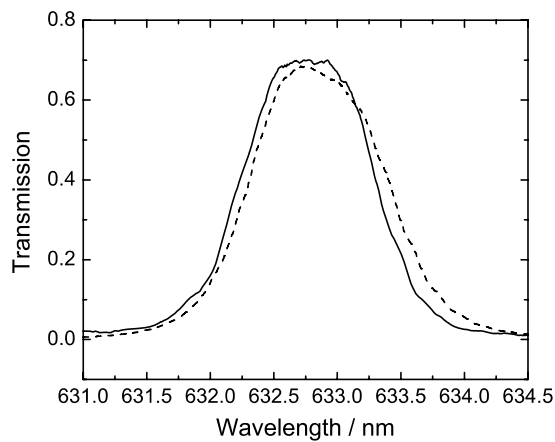


Fig. 3 Comparison of the filter transmission curve measured using the tunable organic semiconductor laser (*solid*) and the Cary 5 photometer (*dashed*). Both measurements were baseline and zero corrected

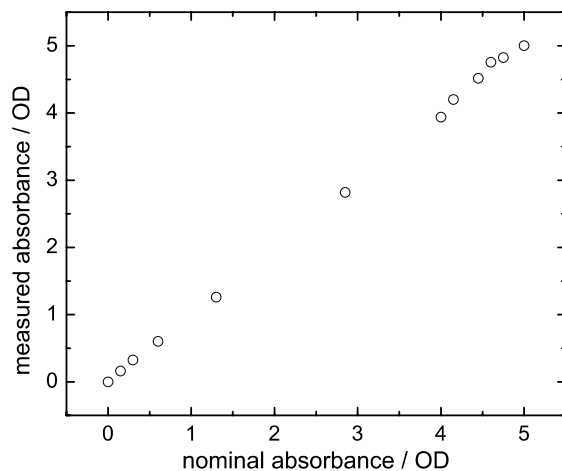


Fig. 4 Relation between the nominal absorbance of non-reflecting neutral density optical filters to the value measured using the organic semiconductor laser based transmission spectrometer

sorbance of different non-reflecting neutral density optical filters at a fixed wavelength of 632 nm. As shown in Fig. 4, we were able to measure optical density (OD) values up to 5 with a maximum error of $OD \pm 0.02$ below and ± 0.2 above values of OD 4. These measurements were mainly limited by the 50:50 beam splitter causing the reference diode to saturate at high pump pulse energies. Using a variable wavelength independent beam splitter, as is common in standard photospectrometer systems, would allow us to measure even higher absorbance values. The applied detection scheme evaluates single laser pulses. The number of transmission spectra which can be measured with the organic laser sample is therefore directly connected to the number of pump laser pulses the sample can be exposed to before degradation. A long-term measurement of the laser emission intensity is plotted in Fig. 5. The sample could be exposed to

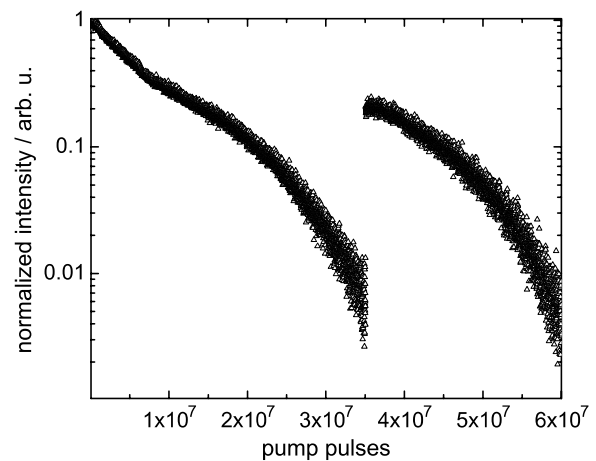


Fig. 5 Laser emission intensity of the encapsulated device in relation to the number of pump pulses. Constant pump pulse energy was used. The operating lifetime is more than 20 million pump pulses

more than 20 million pump pulses at a constant pump energy level. For our transmission measurements we averaged over 64 pulses. Thus, an operational lifetime of more than 100 000 repetitive measurements is already realistic with the existing devices. The degradation can be compensated with an increased pump energy level, thus yielding an even longer lifetime. The shelf life of our device was six months. Further improvements can be anticipated when more advanced organic semiconductor materials are used.

3 Improved wavelength tuning

The tuning scheme utilized in our measurements discussed above was based on a linear positioning stage to move the DFB laser sample relative to the pump laser in order to change the pump position while maintaining a coaxial output beam. Although it seems to be straightforward, this linear tuning method might not be the optimal solution for many applications. The main reason is the micrometer translation system causing the worst case wavelength access time to increase linearly with the tuning range. Our DFB laser sample has an emission wavelength gradient of approx. 30 nm/cm. For a device covering the whole visible spectrum, a wavelength span of 400 nm and thus a translation range of 14 cm would be needed. A fast translation stage with a speed of 50 cm/s and an acceleration of 5 g [18] would need 380 ms from end to end. Besides the extensive hardware costs involved, this is not practical for applications requiring fast scanning at multiple wavelengths. We solved this problem by mounting the DFB laser on a spinning disc and excited it using time-synchronized pump laser light pulses. This tuning method enables high-speed tuning with worst case wavelength access times below 10 ms independently of the tuning gradient. It has very low hardware

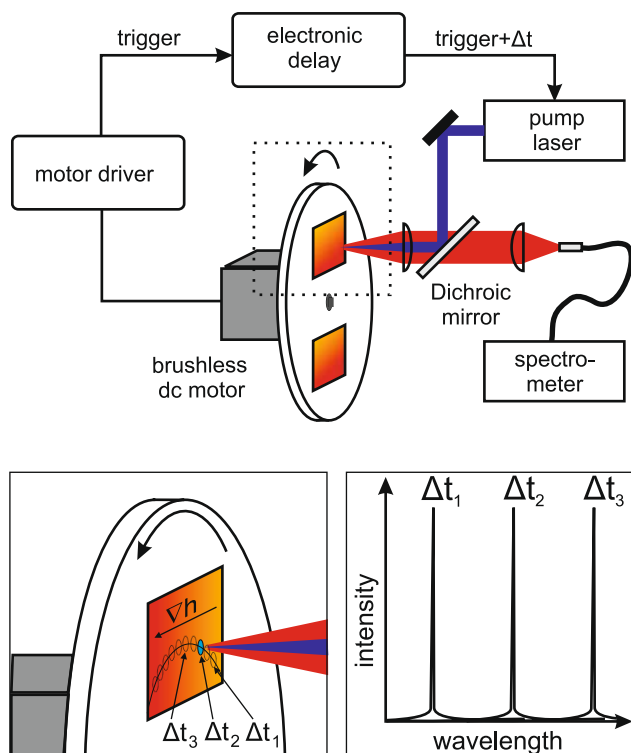


Fig. 6 Schematic of the optical setup. With every revolution of the laser mounting disc the motor driver generates a signal which triggers the pump laser after a variable delay. Different delay times cause the pump laser pulse to excite different regions of the DFB laser sample. As these regions are oriented along the thickness gradient ∇h of the active material layer thickness, the sample emits at different wavelengths

requirements while being comparable to a linear tuning approach regarding accuracy in wavelength selection and long-term wavelength drift. For the experiment, we used a second DFB laser sample. This sample featured a wavelength gradient of 10 nm/cm. It was mounted off axis on a disc with a dummy glass substrate mounted on the opposite side in order to balance masses. To prevent further imbalances, we chose not to encapsulate the sample. For the rotation of the laser mount we used a brushless DC motor (ESky EK5-0002B), which is normally used for model aircraft. An 8-bit RISC microcontroller (Atmel ATMEGA8) based motor driver stage commutates the motor phases with back electromagnetic force (EMF) sensing [19] using a virtual neutral point. A standard triple half-bridge setup is used for the motor power stage. The rotational speed is controlled by pulse-width modulating the phase currents. Due to the back EMF sensing the system operates in a closed loop, providing a very stable rotational speed. A schematic of our experimental setup is depicted in Fig. 6. The motor driver generates a trigger signal at every revolution of the rotating disc. This trigger signal is electronically delayed using a second 8-bit microcontroller system. The delayed signal is then used to trigger an actively Q-switched frequency-tripled Nd:YVO₄ (ACE, AOT) pump laser. This laser emits

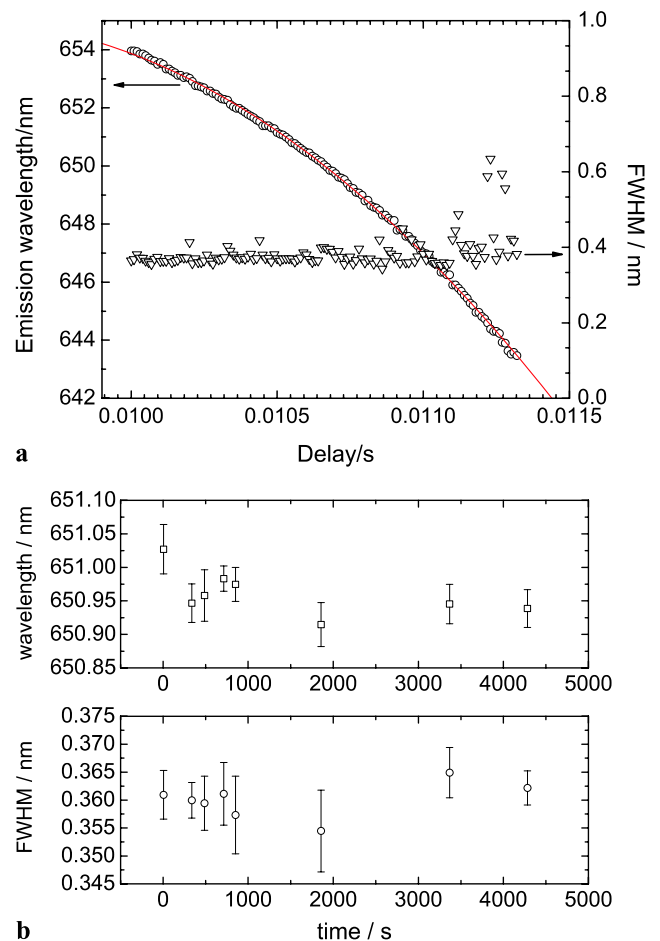


Fig. 7 (a) Tuning of the laser emission wavelength by increasing the delay time in 10- μ s steps. (b) Accuracy and long-term stability of the electronic setup. The data points and error bars have been determined by averaging 15 measurements each

pulses with a wavelength of 355 nm and 500-ps duration. The optical excitation and detection setup is described in more detail in [10]. By varying the electronic delay we were able to excite a discrete position on a circular path with a radius of 2.5 cm on the DFB laser sample and therefore to tune its emission wavelength. Figure 7a shows the measured relations between the delay time and the organic laser emission wavelength and the laser spectral line width, respectively, for a rotation frequency of 75 Hz. The jitter of the pump laser to the external trigger is less than 0.5 ns and can be neglected regarding the 2 μ s (two clock cycles) jitter of the delay generator. This jitter is one-fifth of the average delay time step size required to change the wavelength by 0.1 nm. Thus, the stable long-term operation of our system is evident from Fig. 7b. We measured the emission wavelength and the spectral line width over a period of 70 min while keeping the delay time constant. The measured variations are well inside the range of the achievable resolution of the spectrometer (see above).

4 Conclusion

We demonstrated the applicability of organic semiconductor lasers for high-resolution optical transmission spectroscopy. For this we measured the transmission of a narrow band laser line filter in an optical setup using an encapsulated continuously tunable organic semiconductor laser and a few standard optical components combined with a simple photodiode detection scheme. To evaluate the quality, our measurements were compared with the results obtained by a Cary 5 photospectrometer. Considering the achievable measurement accuracy, we found a good agreement. Instead of using a spectrometer for the calibration of the system in the field the transmission characteristics of known narrow band notch filters can be used for calibration. Additionally, we showed that organic semiconductor lasers are capable of emitting pulses which are sufficient to accurately measure at absorbance values up to OD 5. We have extended the applicability of our system by a novel tuning scheme based on a sub-100\$ hardware solution. Wavelength access times of 10 ms were achieved, irrespective of the wavelength. Our system can easily be extended to cover the whole visible-wavelength spectrum. The laser devices showed lifetimes of more than 20 million pump pulses. The measurement sensitivity and dynamic range can even be improved further by using integrated lock-in detection systems and amplifiers with automatic gain control together with a variable beam splitter. Together with the possibility of using a gallium nitride laser diode for optical pumping, organic semiconductor laser based spectroscopy systems have the potential to be a compact and low-cost alternative to conventional spectroscopic systems in the visible-wavelength region.

Acknowledgements This work was financially supported by the Agilent Technology Foundation. The authors further acknowledge support of the Deutsche Forschungsgemeinschaft (DFG) and the State of Baden-Württemberg through the DFG Center for Functional Nanostructures (CFN) within subproject A 5.5. Mr. Klinkhammer would like

to thank the Karlsruhe School of Optics and Photonics for general support.

References

1. H. Kogelnik, C.V. Shank, *Appl. Phys. Lett.* **18**, 152 (1971)
2. I.D.W. Samuel, G.A. Turnbull, *Chem. Rev.* **107**, 1272 (2007)
3. S.R. Forrest, *Nature* **428**, 911 (2004)
4. M. Stroisch, T. Woggon, U. Lemmer, G. Bastian, G. Violakis, S. Pissadakis, *Opt. Express* **15**, 3968 (2007)
5. D. Pisignano, L. Persano, P. Visconti, R. Cingolani, G. Gigli, G. Barbarella, L. Favaretto, *Appl. Phys. Lett.* **83**, 2545 (2003)
6. V.G. Kozlov, V. Bulovic, P.E. Burrows, M. Baldo, V.B. Khalfin, G. Parthasarathy, S.R. Forrest, Y. You, M.E. Thompson, *J. Appl. Phys.* **84**, 4096 (1998)
7. U. Scherf, S. Riechel, U. Lemmer, R.F. Mahrt, *Curr. Opin. Solid State Mater. Sci.* **5**, 143 (2001)
8. S. Riechel, U. Lemmer, J. Feldmann, S. Berleb, A.G. Mückl, W. Brütting, A. Gombert, V. Wittwer, *Opt. Lett.* **26**, 592 (2001)
9. D. Schneider, T. Rabe, T. Riedl, T. Dobbertin, M. Kröger, E. Becker, H.-H. Johannes, W. Kowalsky, T. Weimann, J. Wang, P. Hinze, *Appl. Phys. Lett.* **85**, 1886 (2004)
10. S. Klinkhammer, T. Woggon, U. Geyer, C. Vannahme, S. Dehm, T. Mappes, U. Lemmer, *Appl. Phys. B* **97**, 787 (2009)
11. C. Karnutsch, M. Stroisch, M. Punke, U. Lemmer, J. Wang, T. Weimann, *IEEE Photonics Technol. Lett.* **19**, 741 (2007)
12. T. Riedl, T. Rabe, H.-H. Johannes, W. Kowalsky, J. Wang, T. Weimann, P. Hinze, B. Nehls, T. Farrell, U. Scherf, *Appl. Phys. Lett.* **88**, 241116 (2006)
13. Y. Yang, G.A. Turnbull, I.D.W. Samuel, *Appl. Phys. Lett.* **92**, 163306 (2008)
14. M. Punke, T. Woggon, M. Stroisch, B. Ebenhoch, U. Geyer, C. Karnutsch, M. Gerken, U. Lemmer, M. Bruendel, J. Wang, T. Weimann, *Proc. SPIE* **6659**, 665909 (2007)
15. U. Geyer, J. Hauss, B. Riedel, S. Gleiss, U. Lemmer, M. Gerken, *J. Appl. Phys.* **104**, 093111 (2008)
16. S. Riechel, U. Lemmer, J. Feldmann, T. Benstem, W. Kowalsky, U. Scherf, A. Gombert, V. Wittwer, *Appl. Phys. B* **71**, 897 (2000)
17. D. Anderson, M. Archard, *Varian UV Instrum. Work UV-94* (1992)
18. S. Jordan, *Laser Focus World* **44**(9) (2008)
19. K. Iizuka, H. Uzuhashi, M. Kano, T. Endo, K. Mohri, *IEEE Trans. Ind. Appl.* **IA-21**, 595 (1985)